Reprinted From . . .

CHEMICAL ENGINEERING COMPUTING WORKSHOP

STOCHASTIC GREEN'S FUNCTION METHOD FOR CALCULATING THE CONCENTRATION PROFILE OF A CHEMICALLY REACTIVE SPECIES

C. E. Wyman and M. D. Kostin

Department of Chemical Engineering
Princeton University, Princeton, New Jersey

Vol. 1, No. W4

Pages 32-34

RESEARCH:

Stochastic Green's Function Method for Calculating the Concentration Profile of a Chemically Reactive Species

C. E. Wyman and M. D. Kostin

Department of Chemical Engineering
Princeton University
Princeton, New Jersey

A Green's function formalism is used to derive a stochastic method for calculating the concentration profile of a chemically reactive species subjected to diffusion and a convective velocity field. The validity of the stochastic method is investigated by calculating the exact solution for the concentration profile of a reactive species in a laminar flow tubular reactor and comparing it with the profile obtained from the random walk of the stochastic method. The agreement is found to be excellent. As an example of its application, the stochastic Green's function method is used to estimate the time-dependent concentration of a solute for a three-dimensional convective diffusion problem.

In the numerical solution of the three-dimensional convective diffusion equation for a chemically reactive species, a major difficulty arises from the very large number of mesh points that must be treated. For example, if the x, y, and z directions have a grid of 40 mesh points each, then the three-dimensional problem involves a grid of 64,000 mesh points. The demands made on computer memory and on computer time by a conventional finite-difference approach with this large number of mesh points lead to serious practical problems. Such difficulties are present, for example, in the calculation of the distribution of pollutants (*1*). However, if only an estimate of the distribution of the chemically reactive species is required, then the stochastic, or Monte Carlo, method (*2–4*) may be extremely helpful. The stochastic method has been used, for example, to calculate the wave function of the Schrodinger equation (*5–8*), to study the convective diffusion of solutes (*9, 10*), to calculate the energy distribution of a chemically reactive species (*11, 12*), and to obtain transport coefficients of electrons in gases (*13*). This paper presents a stochastic method based on the Green's function for solving the convective diffusion equation for a chemically reactive species in three spatial dimensions. To establish the validity of the stochastic Green's function method, the concentration profile of a reactive species in a viscous flow tubular reactor is calculated by a finite-difference method and compared with the stochastic result. The agreement is found to be excellent.

STOCHASTIC GREEN'S FUNCTION

The time-dependent convective diffusion equation for a chemically reactive species is given as

$$\frac{\partial C}{\partial t} = D\nabla_{\mathbf{r}}^2 C - \mathbf{v}(\mathbf{r})\cdot\nabla_{\mathbf{r}} C - k(\mathbf{r})C(\mathbf{r}, t) \qquad (1)$$

where $C(\mathbf{r}, t)$ is the concentration of the chemically reactive species, D is the diffusivity, $\mathbf{v}(\mathbf{r})$ is the convective velocity field, and $k(\mathbf{r})$ is the rate constant for a first-order reaction. The concentration of the chemically reactive species at time t can be obtained from that at time t' from the equation

$$C(\mathbf{r}, t) = \iiint G(\mathbf{r}, t; \mathbf{r}'t')C(\mathbf{r}', t')dV' \qquad (2)$$

where Green's function $G(\mathbf{r}, t; \mathbf{r}'t')$ is a solution of

$$\frac{\partial G}{\partial t} = D\nabla_{\mathbf{r}}^2 G - \mathbf{v}(\mathbf{r})\cdot\nabla_{\mathbf{r}} G - k(\mathbf{r})G(\mathbf{r}, t; \mathbf{r}', t') + \delta(\mathbf{r}-\mathbf{r}')\delta(t-t') \qquad (3)$$

Since the convective velocity field $\mathbf{v}(\mathbf{r})$ and the rate constant $k(\mathbf{r})$ are in general complicated functions of position, solutions of Equation (3) are extremely difficult to obtain. However, if we consider the case where t is slightly larger than t', then we would expect the reactive species to be concentrated in the region around $\mathbf{r}'$. In mathematical terms, $G(\mathbf{r}, t; \mathbf{r}', t')$ would have a large value for $\mathbf{r} \approx \mathbf{r}'$ and would be essentially zero elsewhere. For this case ($t \approx t'$), the solution of Equation (3) is determined by the values of $\mathbf{v}(\mathbf{r})$ and $k(\mathbf{r})$ near $\mathbf{r}'$ and is essentially independent of the values of $\mathbf{v}(\mathbf{r})$ and $k(\mathbf{r})$ far from $\mathbf{r}'$. Thus we would expect that

$$G(\mathbf{r}, t; \mathbf{r}', t) \approx H(\mathbf{r}, t; \mathbf{r}', t') \quad t \approx t' \qquad (4)$$

where $H(\mathbf{r}, t; \mathbf{r}', t')$ is a solution of

$$\frac{\partial H}{\partial t} = D\nabla_r^2 H - \mathbf{v}(\mathbf{r}')\cdot\nabla_r H - k(\mathbf{r}')H(\mathbf{r}, t; \mathbf{r}', t') + \delta(\mathbf{r}-\mathbf{r}')\delta(t-t') \quad (5)$$

Since the coefficients of Equation (5) are not functions of the independent variable $\mathbf{r}$, a solution can be derived. Using a transformation discussed by Jost (*14*), we obtain

$$H(\mathbf{r}, \mathbf{r}') = (\beta/\pi)^{3/2} \exp\{-\beta(\mathbf{r}-\mathbf{r}'-\mathbf{v}(\mathbf{r}')/4D\beta)^2\} \exp\{-k(\mathbf{r}')/4D\beta\} \quad (6)$$

where

$$\beta = 1/4(t-t')D \quad (7)$$

A set of points whose distribution is given by the Green function of Equation (6) can easily be generated from random numbers supplied by the computer. The procedure consists of displacing the point from position $\mathbf{r}'$ to position $\mathbf{r}'+\mathbf{v}(\mathbf{r}')/4D\beta$ and then using three Gaussian distributed random numbers with a variance of $1/2\beta$ to determine the final x, y, and z components of displacement. A fourth random number R_n, whose distribution is uniform between zero and unity, is next compared with the value of $\exp\{-k(\mathbf{r}')/4D\beta\}$. If $R_n > \exp\{-k(\mathbf{r}')/4D\beta\}$ then a reaction is said to have occurred and the point is deleted. If $R_n < \exp\{-k(\mathbf{r}')/4D\beta\}$, then the point is retained. This subprogram, which relates random numbers supplied by the computer to displacements whose distribution is given by Equation (6), is used to generate a random walk of representative molecules of the chemically reactive species. By preparing a histogram of the positions of many molecules, a concentration profile of the chemically reactive species is obtained.

To test the validity of using the Green function given by Equation (6) in the stochastic method instead of the extremely complicated Green function that is a solution of Equation (3), we compared the concentration profile obtained using the stochastic method with an exact solution. Since exact analytical or numerical solutions to a full three-dimensional problem involving convection, diffusion, and chemical reaction are rare and difficult to obtain, we chose a two-dimensional case. The problem selected was the classical experimental and numerical study of Cleland and Wilhelm (*15*), who undertook a thorough investigation of the laminar flow tubular reactor. The experimental reaction studied was the hydrolysis of acetic anhydride, a reaction that lends itself to theoretical study because it appears to be first order in the anhydride when performed in excess water. The convective diffusion equation that they treated is

$$D\left[\frac{\partial^2 C}{\partial r^2} + \frac{1}{r}\frac{\partial C}{\partial r}\right] - [1-(r/R)^2]v_0\frac{\partial C}{\partial z} - kC = 0 \quad (8)$$

where R is the radius of the tube and v_0 is the velocity of the center streamline. The Crank-Nicholson method was used with Equation (8) to obtain numerical solutions for the concentration profile of the reactive species. The numerical accuracy of these results was checked by increasing the number of mesh points until we found that further increases had no effect on the results.

The effluent concentration, which is an integral average concentration based on the volumetric flow rate, is defined as

$$C_e(z) = \frac{\int_0^R 2\pi r v(r)\, C(r, z)dr}{\int_0^R 2\pi r v(r)dr} \quad (9)$$

Another quantity, the mean concentration, is defined as

$$C_m(z) = \frac{\int_0^R 2\pi r\, C(r, z)dr}{\int_0^R 2\pi r dr} \quad (10)$$

In Figure 1 four sets of data for a laminar flow tubular reactor are shown. The broken line is the Crank-Nicholson solution of Equation (8) for the effluent concentration $C_e(Z)$ as a function of the dimensionless axial distance $Z = z/R$, and the squares give the results for a long stochastic run for the same case. The close agreement between these two results indicates the validity of the stochastic method. The solid line is the Crank-Nicholson solution of Equation (8) for the mean concentration $C_m(Z)$, and the circles give the stochastic result for the same case. Again, the agreement is excellent. Additional data that were obtained for other values of the parameters α and V_0 showed similar agreement, supporting the thesis of the validity of the stochastic method.

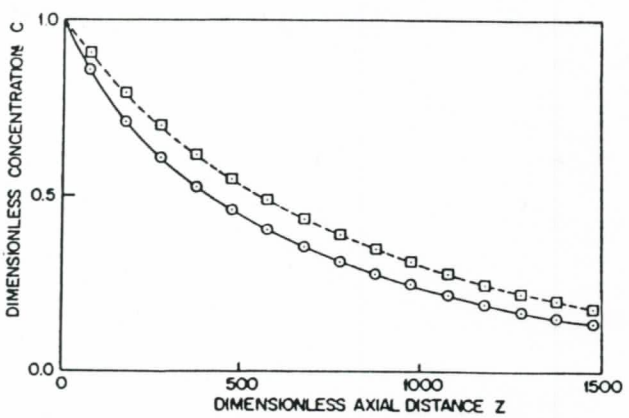

Figure 1. Dimensionless concentration versus dimensionless axial distance for a laminar flow tubular reactor with $\alpha = D/kR^2 = 0.036$ and $V_0 = v_0/kR = 1400$. The broken line is the Crank-Nicholson solution for the effluent concentration $C_e(Z)$ as a function of the dimensionless axial distance $Z = z/R$, and the squares give the stochastic result for the same case. The solid line is the Crank-Nicholson solution for the mean concentration $C_m(Z)$ and the circles give the stochastic result for the same case.

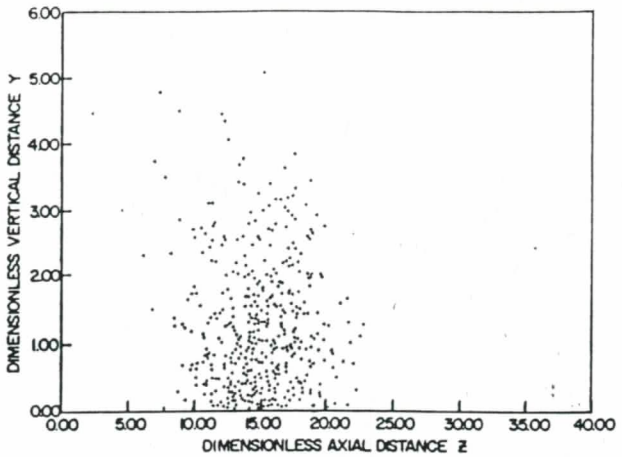

Figure 2. Dimensionless Y and Z coordinates of representative solute molecules at dimensionless time $T = 20$ in a slit with $\gamma = 0.05$. Each point gives the $Y-Z$ position of a representative solute molecule.

The stochastic Green function method is especially useful when an estimate of the solution to a convective diffusion problem in three dimensions is required. For example, consider a thin slit whose walls are perpendicular to the x axis and intersect the x axis at $x = -a$ and $x = +a$. The streamlines are given as parallel to the z axis and the convective velocity field is

$$\mathbf{v}(\mathbf{r}) = [1-(x/a)^2]v_0\mathbf{e}_z \qquad (11)$$

where $\mathbf{e}_z$ is a unit vector in the z direction. At time $t = 0$, a pulse of solute is injected into the system at position $\mathbf{r}_s = (x_s, y_s, z_s)$, and we wish to determine the spatial distribution of solute at a time t later. For simplicity, we consider the case of no reaction ($k = 0$). The convective diffusion equation for these conditions has the form

$$\frac{\partial C}{\partial t} = D\left[\frac{\partial^2 C}{\partial x^2} + \frac{\partial^2 C}{\partial y^2} + \frac{\partial^2 C}{\partial z^2}\right] - [1-(x/a)^2]v_0\frac{\partial C}{\partial z} + \delta(\mathbf{r}-\mathbf{r}_s)\delta(t) \qquad (12)$$

It is convenient to use the dimensionless spatial variables

$$X = x/a \qquad Y = y/a \qquad Z = z/a \qquad (13)$$

the dimensionless time

$$T = tv_0/a \qquad (14)$$

and the dimensionless parameter

$$\gamma = D/v_0a \qquad (15)$$

Solutions of this three-dimensional equation by standard numerical methods using finite differences are difficult to obtain because the gradients are steep and the number of mesh points needed is very large. However, with the stochastic method, use of Green's function of Equation (6) to generate a random walk readily gives the positions of representative solute molecules at time t. Instead of preparing a histogram,

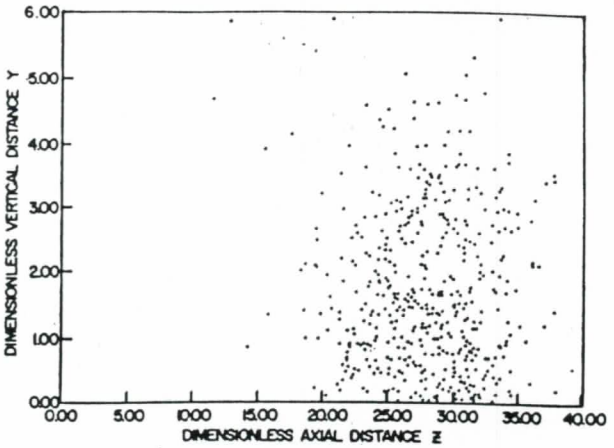

Figure 3. Dimensionless Y and Z coordinates of representative solute molecules at dimensionless time $T = 40$ in a slit with $\gamma = 0.05$. Each point gives the $Y-Z$ position of a representative solute molecule.

it is sometimes more convenient to plot the positions of the solute molecules. This can be done automatically with a Calcomp plotter.

In Figure 2 are shown the dimensionless Y and Z coordinates of representative solute molecules at dimensionless time $T = 20$. The solute molecules are introduced into the system at $T = 0$ at position $X_s = 1$, $Y_s = 0$, $Z_s = 2$. Only one-half of the full distribution, which is symmetric with respect to the X-Z plane at $Y = 0$, is shown. The coordinates of the solute molecules at a later dimensionless time of $T = 40$ are given in Figure 3. More than 20 such histories can be obtained on an IBM 360/91 in less than 4 sec. of execution time.

ACKNOWLEDGMENT

We would like to thank D. F. Bruley for helpful discussions, and the National Science Foundation for its support of this research. In addition, this work made use of computer facilities supported in part by National Science Foundation Grants NSF-GJ-34 and NSF-GU-3157.

REFERENCES

1. Ross, L. W., *Simulation*, **14**, 165 (1970).
2. Cashwell, E. D., and C. J. Everett, *The Monte Carlo Method for Random Walk Problems*, Pergamon Press, New York (1969).
3. Hammersley, J. M., and D. C. Handscomb, *Monte Carlo Methods*, Wiley, New York (1964).
4. Shreider, Yu. A., *The Monte Carlo Method*, Pergamon Press, Oxford (1966).
5. Donsker, M. D., and M. Kac, *J. Res. Natl. Bur. Std.*, **44**, 551 (1950).
6. Fortet, R., *J. Res. Natl. Bur. Std.*, **48**, 68 (1952).
7. Metropolis, N., in *Symposium on Monte Carlo Methods*, p. 29, Interscience, New York (1956).
8. Kostin, M. D., and K. Steiglitz, *Phys. Rev.*, **159**, 27 (1967).
9. Bugliarello, G., and E. D. Jackson III, *J. Eng. Mech. Div.*, **90** (EM4), 49 (Aug. 1964).
10. Bugliarello, G., and J. W. Hoskins, in Proc. 19th Ann. Conf. Eng. Med. Biol. (1966).
11. Chapin, D. C., and M. D. Kostin, *J. Chem. Phys.*, **48**, 3067 (1968).
12. Chapin, D. C., and M. D. Kostin, *J. Chem. Phys.*, **52**, 5317 (1970).
13. Bell, M. J., and M. D. Kostin, *Phys. Rev.*, **169**, 150 (1968).
14. Jost, W., *Diffusion*, p. 47, Academic Press, New York (1960).
15. Cleland, F. A., and R. H. Wilhelm, *AIChE J.*, **2**, 489 (1956).

Reprinted from:

THE JOURNAL OF CHEMICAL PHYSICS VOLUME 59, NUMBER 6 15 SEPTEMBER 1973

Anomalous osmosis: Solutions to the Nernst–Planck and Navier–Stokes equations*

C. E. Wyman and M. D. Kostin

Department of Chemical Engineering, Princeton University, Princeton, New Jersey 08540

(Received 19 April 1973)

The phenomenon of anomalous osmosis is studied by using the coupled Nernst–Planck and Navier–Stokes equations to investigate diffusion of an electrolyte through a pore of an ion-exchange membrane. Exact solutions to these equations show that a concentration gradient can produce fluid motion. It is found that the velocity profiles may be significantly different from those of Poiseuille flow.

I. INTRODUCTION

When a membrane impermeable to a nonionic solute separates two nonelectrolytic solutions of different concentrations, the flow of solvent is termed osmosis and van't Hoff's law holds. When an ion-exchange membrane separates two electrolytic solutions of different concentrations, deviations from van't Hoff's law occur and the phenomenon is called anomalous osmosis.[1,2] A theory of anomalous osmosis, based on approximate solutions to the Nernst–Planck equations, has been presented by Schlögl.[1,3] Kobatake and his colleagues[4–9] have studied the Navier–Stokes equations coupled to the flux equations of the Nernst–Planck equations or to the flux equations of irreversible thermodynamics. In their work they introduced simplifying assumptions regarding the velocity profile, such as that the velocity profile was parabolic or that the velocity profile was independent of axial distance. It is the purpose of this paper to develop more detailed and precise results by obtaining exact solutions to the Nernst–Planck and Navier–Stokes equations for an electrolyte in a pore of an ion-exchange membrane. The exact solutions show that the velocity profiles in a cylindrical capillary of an ion-exchange membrane may show substantial deviations from those of Poiseuille flow and may depend markedly on axial distance.

II. DIFFUSION AND HYDRODYNAMIC EQUATIONS

The time-independent Navier–Stokes equation for a fluid of constant density ρ and viscosity μ is

$$\rho \mathbf{w}\cdot\nabla\mathbf{w} = \mathbf{f} - \nabla P + \mu\nabla^2\mathbf{w}, \tag{1}$$

where $\mathbf{w}$ is the fluid velocity, $\mathbf{f}$ is the force per unit volume, and P is the pressure. The hydrodynamic continuity equation is

$$\nabla\cdot\mathbf{w} = 0. \tag{2}$$

For a cylindrical pore of radius R and length L, Eqs. (1) and (2) have the form

$$\rho\left(v_r\frac{\partial v_r}{\partial r} + v_z\frac{\partial v_r}{\partial z}\right) = f_r - \frac{\partial P}{\partial r} + \mu\left(\frac{\partial^2 v_r}{\partial r^2} + \frac{1}{r}\frac{\partial v_r}{\partial r} - \frac{v_r}{r^2} + \frac{\partial^2 v_r}{\partial z^2}\right), \tag{3}$$

$$\rho\left(v_r\frac{\partial v_z}{\partial r} + v_z\frac{\partial v_z}{\partial z}\right) = f_z - \frac{\partial P}{\partial z} + \mu\left(\frac{\partial^2 v_z}{\partial r^2} + \frac{1}{r}\frac{\partial v_z}{\partial r} + \frac{\partial^2 v_z}{\partial z^2}\right), \tag{4}$$

$$(\partial v_r/\partial r) + (v_r/r) + (\partial v_z/\partial z) = 0, \tag{5}$$

where v_r and v_z are the radial and axial components of fluid velocity, respectively. The boundary conditions for the partial differential equations (3) to (5) involving $v_r(r,z)$, $v_z(r,z)$, and $P(r,z)$ are

$$v_r(R,z) = 0, \tag{6}$$

$$v_z(R,z) = 0, \tag{7}$$

$$v_r(0,z) = 0, \tag{8}$$

$$\partial v_z(0,z)/\partial r = 0, \tag{9}$$

$$v_r(r,0) = 0, \tag{10}$$

$$P(r,0) = P_0, \tag{11}$$

$$v_r(r,L) = 0, \tag{12}$$

$$P(r,L) = P_1, \tag{13}$$

where P_0 and P_1 are the inlet ($z=0$) and outlet ($z=L$) pressures, respectively.

The time-independent Nernst–Planck equations for univalent cations and anions are

$$\Phi_a = -D_a\nabla c_a - (FD_a c_a/R_g T)\nabla\phi, \tag{14}$$

$$\Phi_b = -D_b\nabla c_b + (FD_b c_b/R_g T)\nabla\phi, \tag{15}$$

$$\nabla\cdot\Phi_a = 0, \tag{16}$$

$$\nabla\cdot\Phi_b = 0, \tag{17}$$

where c_a is the number of moles of cations per unit volume, Φ_a is the molar flux of cations, c_b is the number of moles of anions per unit volume, Φ_b is the molar flux of anions, ϕ is the electric

potential, F is Faraday's constant, R_g is the gas constant, and T is the absolute temperature. The diffusion coefficients of the cations (species A) and the anions (species B) are denoted by D_a and D_b, respectively. Poisson's equation relates the electric potential to the concentrations:

$$\nabla^2\phi = -(4\pi F/\epsilon)(c_a - c_b), \tag{18}$$

where ϵ is the permittivity and the terms are expressed in cgs units. The force per unit volume resulting from the electric field is

$$f = -(c_a - c_b)F\nabla\phi. \tag{19}$$

The condition that the molar flux is zero at $r = R$ gives us the boundary conditions

$$[\partial c_a(R,z)/\partial r] + [Fc_a(R,z)/R_gT][\partial\phi(R,z)/\partial r] = 0, \tag{20}$$

$$[\partial c_b(R,z)/\partial r] - [Fc_b(R,z)/R_gT][\partial\phi(R,z)/\partial r] = 0\ . \tag{21}$$

Fixed ionized groups are considered to be distributed on the interior surface of the pore. The boundary condition used for the electric potential at $r = R$ is

$$\partial\phi(R,z)/\partial r = (4\pi/\epsilon)\sigma(z), \tag{22}$$

where $\sigma(z)$ is the surface charge density. At the center line of the pore we have the boundary conditions

$$\partial c_a(0,z)/\partial r = 0, \tag{23}$$

$$\partial c_b(0,z)/\partial r = 0, \tag{24}$$

$$\partial\phi(0,z)/\partial r = 0. \tag{25}$$

At $z = 0$ and $z = L$ the boundary conditions are

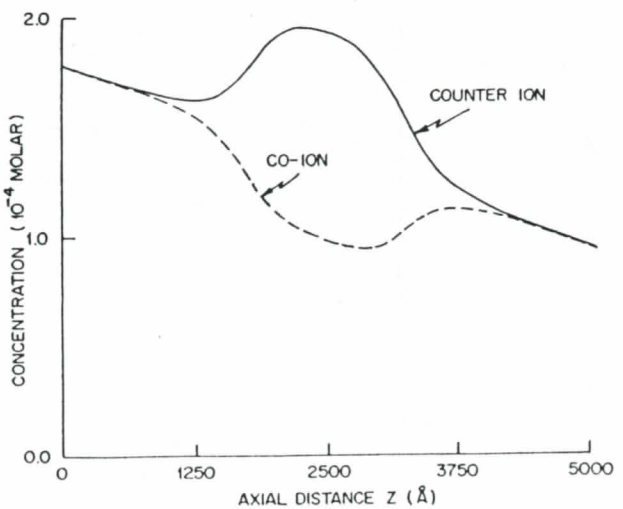

FIG. 1. Concentration of counterion and concentration of co-ion as a function of axial distance at radius r = 750 Å.

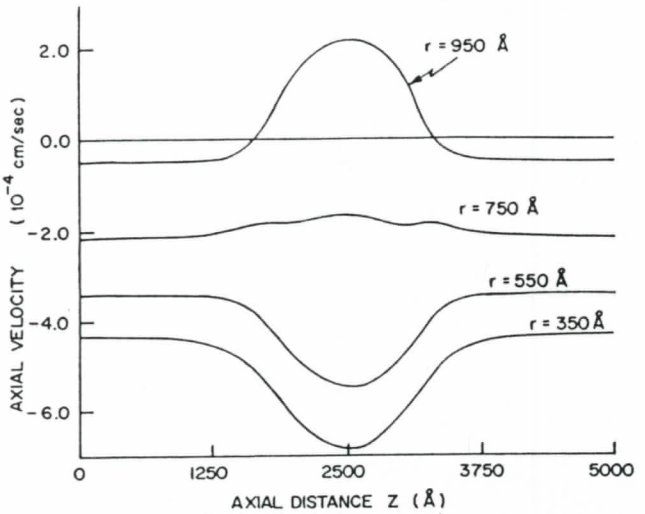

FIG. 2. Axial velocity as a function of axial distance at radii r = 350, 550, 750, and 950 Å.

$$c_a(r,0) = c_0, \tag{26}$$

$$c_b(r,0) = c_0, \tag{27}$$

$$\phi(r,0) = \phi_0, \tag{28}$$

$$c_a(r,L) = c_1, \tag{29}$$

$$c_b(r,L) = c_1, \tag{30}$$

$$\phi(r,L) = \phi_1. \tag{31}$$

III. RESULTS AND DISCUSSION

The partial differential equations (3)–(5) and (14)–(19) with the boundary conditions (6)–(13) and (20)–(31) were solved on a digital computer by the method of finite differences. Test cases were run to confirm the proper operation of the computer program. For example, taking the surface charge density equal to zero, setting the potential difference

$$\Delta\phi = \phi_1 - \phi_0 \tag{32}$$

equal to zero, but letting the pressure difference

$$\Delta P = P_1 - P_0 \tag{33}$$

be different from zero, we obtained the expected parabolic velocity profile (Poiseuille flow) from the computer program.

Next, we considered the distribution of surface charge to be $\sigma(z) = 0$ for $0 < z < z_1$, $\sigma(z) = \sigma_c$ for $z_1 < z < z_2$, and $\sigma(z) = 0$ for $z_2 < z < L$. The pressure difference ΔP and the potential difference $\Delta\phi$ were set equal to zero and the inlet concentration c_1 was set equal to the outlet concentration c_2. For this case we found that no flow occurred and that c_a and c_b were in agreement with the equilibrium Boltzmann distribution. Then, we increased the inlet concentration but kept all other parameters fixed. We found that a concentration gradient produced fluid flow.

In Fig. 1 is shown the concentration of the counterion c_a and the concentration of the co-ion c_b as a function of axial distance at $r = 750$ Å for the following parameters: $c_0 = 1.80 \times 10^{-4}$ M, $c_1 = 0.95 \times 10^{-4} M$, $\Delta P = 0$, $\Delta\phi = 0$, $R = 1000$ Å, $L = 5000$ Å, $z_1 = 1750$ Å, $z_2 = 3250$ Å, $\sigma_c = -145$ statcoulombs/cm^2, $D_a = D_b = 1.95 \times 10^{-5}$ cm^2/sec, $\mu = 1.0 \times 10^{-2}$ g/cm · sec, $\epsilon = 78.5$, $\rho = 1.0$ g/cm^3, and $T = 300$ °K. The increase in the concentration of the positively charged counterions in the vicinity of the negatively charged fixed ions is evident. In the same region, the concentration of the negatively charged co-ions shows a decrease. The deviation from electroneutrality in the neighborhood of the fixed ions is seen to be appreciable. In Fig. 2 is shown the axial velocity v_z as a function of axial distance. The axial velocity at $r = 350$ Å is in a direction opposite to the concentration flux and does not remain constant with axial position but increases in absolute magnitude in the region of the fixed ions. The axial velocity at $r = 950$ Å, which is negative well outside the region of fixed charges, goes to zero and then becomes positive inside the region of fixed charges. Thus, we see that a concentration gradient can produce fluid motion and that the velocity profiles can be quite complex.

*Supported in part by a grant from the National Science Foundation.

[1]F. Helfferich, *Ion Exchange* (McGraw-Hill, New York, 1962), pp. 389 ff.
[2]N. Lakshminarayanaiah, *Transport Phenomena in Membranes* (Academic, New York, 1969), pp. 186 ff.
[3]R. Schögl, Z. Phys. Chem. (Frankf. a. M.) **3**, 73 (1955).
[4]Y. Kobatake, J. Chem. Phys. **28**, 146 (1958).
[5]Y. Kobatake, J. Chem. Phys. **28**, 442 (1958).
[6]Y. Kobatake and H. Fujita, J. Chem. Phys. **40**, 2212 (1964).
[7]Y. Kobatake and H. Fujita, J. Chem. Phys. **41**, 2963 (1964).
[8]Y. Kobatake and H. Fujita, Kolloid-Z. **196**, 58 (1964).
[9]Y. Kobatake, N. Takeguchi, Y. Toyoshima, and H. Fujita, J. Phys. Chem. **69**, 3981 (1965).